JP1J.14 DIFFERENCES BETWEEN EXPLICIT AND APPROXIMATED RADAR RAY PATHS DUE TO THE VERTICAL GRADIENT OF REFRACTIVITY

Jidong Gao[1], Keith Brewster[1] and Ming Xue[1,2]
[1]Center for Analysis and Prediction of Storms and
[2]School of Meteorology
University of Oklahoma

1. INTRODUCTION

The United States operational WSR-88D Doppler radar radar network (NEXRAD) is becoming increasingly important for improving the real time detection and warning of hazardous weather (Alberty et al. 1991; Crum et al. 1998; Serafin and Wilson 2000). It is viewed as an essential observing system for initializing non-hydrostatic, storm-resolving (i.e., horizontal grid spacing of order 1 km) numerical weather prediction (NWP) models (e.g., Lilly, 1990; Droegemeier, 1990, 1997). Attempts to demonstrate such capability began early in the past decade (e.g., Sun et al., 1991), and subsequent efforts have been notably successful (e.g., Gao et al. 1998; Weygandt et al. 2002a,b; Crook and Sun 2002; Xue et al. 2003; Brewster et al. 2003; Gao et al. 2004, Hu et al. 2005a,b).

To assimilate the radar reflectivity and radial velocity data from weather radar into an NWP model, it is necessary to use suitable ray path equations to obtain the physical location of each radar measurement and to have accurate forward operators to convert model winds to radial velocity in data assimilation schemes. Currently, there are several versions of ray path equations in the textbooks (e. g., Doviak and Zrnic 1993). Most early studies on radar data assimilation use a simple ray path equation in the forward operator that projects the wind vectors from a model grid to the radial direction, such as the one based on the Cartesian flat-earth geometry, (e.g., Gao et al. 1998, 2005; Shapiro et al. 2003; Weygandt et al. 2002a,b). The next level of sophistication is to use the four-thirds earth radius model for the radar ray path calculations (e.g., Brewster, 2003). This model takes into account the curvature of the earth and the average refractivity gradient in the atmosphere. It, however, assumes that the atmosphere has a constant vertical gradient of refractivity in the lower troposphere, as determined from the standard atmosphere. In reality, the gradient of the refractivity is seldom constant, and significant departures from the linearity assumption exist when there are strong temperature inversions and/or large vertical moisture gradients. A better understanding of the sensitivity of the ray path to the actual gradients of refractivity and of the frequency that significant departures occur from the prediction of simple models is valuable to radar data quality control and radar data assimilation. In this study, the sensitivity of radio refractivity to temperature and moisture is first analyzed and the influence of atmospheric radio refractivity on the ray paths at selected geographical locations in the United States is then examined using several years of sounding data from National Weather Service.

The rest of this paper is organized as follows. In Section 2, the four-thirds earth radius model, used for the radar ray path calculations, is briefly reviewed. An analysis of the sensitivity of refractivity to temperature and moisture variables is given in Section 3. In Section 4, a stepwise ray trace method is introduced. The influence of atmospheric refractivity on the ray path at different geographical locations in the United States is examined using historic sounding data from National Weather Service in Section 5. Finally, a summary and conclusions are given in Section 6.

2. THE RAY PATH EQUATIONS

Under the assumption that temperature and humidity are horizontally homogeneous so that refractivity is a function only of height above ground, a formula can be derived that expresses the ray path in terms of a curve following a sphere of radius (Doviak and Zrnic 1993),

$$a_e = \frac{a}{1 + a\left(dn/dh\right)} = k_e a \,, \tag{1}$$

where *a* is the earth's radius and k_e is a multiplier which is dependent on the vertical gradient of refractive index of air, *dn/dh*. When the Standard Atmosphere is considered, it is found that k_e is equal to 4/3. This is often referred to as the "four-thirds earth radius model". The refractive index of air, *n*, is a function of its temperature, pressure

and humidity and is usually taken, subject to certain assumptions, as (Beam and Dutton 1968),

$$N = (n-1)\times 10^6 = 77.6P/T + 3.73\times 10^5 eT^{-2} \quad (2)$$

where *P* is air pressure in hPa (including water vapor pressure), *e* is water vapor pressure in hPa, and *T* is air temperature in degrees K. It is convenient to use the quantity *N,* the atmosphere radio refractivity, instead of *n*. *N* represents the departure of *n* from unity in parts per million. *N* typically has a value of about 300 near the ground surface and its variations with the height, *dN/dh*, can be considered more conveniently.

The following two equations relate the height above ground, *h,* and the surface range (distance along the earth's surface from radar), *s*, to radar-measurable parameters, the slant path, *r* and radar elevation angle, θ_e (Doviak and Zrnic 1993),

$$s = a_e \sin^{-1}\left(\frac{r\cos\theta_e}{a_e + h}\right), \quad (3)$$

$$h = \left[r^2 + a_e^2 + 2ra_e \sin\theta_e\right]^{1/2} - a_e . \quad (4)$$

In the same text it is also shown that if $r \ll k_e a$, the coordinates *x, y* and *z* are related to the radar coordinates (r, θ_e, ϕ) by,

$$x \approx r\cos\theta_e' \sin\phi , \quad (5a)$$

$$y \approx r\cos\theta_e' \cos\phi , \quad (5b)$$

$$z = h = (a_e^2 + r^2 + 2rk_e a\sin\theta_e')^{1/2} - k_e a , \quad (5c)$$

where θ_e', the angle between the radar beam and the tangent plane below the data point, is the sum of two terms expressed as the following,

$$\theta_e' = \theta_e + \tan^{-1}[r\cos\theta_e /(a_e + r\sin\theta_e)] . \quad (6)$$

From (5a) and (5b), one can easily derive the distance along the earth's surface as,

$$s' \approx r\cos\theta_e' . \quad (7)$$

Equation (7) is an approximation of the ray path equation (3). Equation (5c) uses exactly the four-thirds earth radius beam height equation (4).

3. SENSITIVITY ANALYSIS OF REFRACTIVITY TO TEMPERATURE AND DEWPOINT

In equation (2), the first term on the right hand side is known as the dry term, the second term is the moist term. The value of radio refractivity *N* can be computed from measurements of pressure, *P,* temperature, *T,* and water vapor, *e*. Because in the troposphere the fractional decrease in *P* is larger than that for *T*, the variation of radio refractivity *N* with height, *dN/dh*, is usually negative. For the Standard Atmosphere, *dN/dh* is about –39.2 km^{-1}. If *N* decreases more (less) rapidly with height than the Standard Atmosphere, the beam may be refracted more (less), and in such cases, the height of a target may be overestimated (underestimated) by the four-thirds earth radius model. In an extreme condition, e.g., in the presence of a sharp refractivity gradient of about –150 km^{-1} below 100 m above ground level, a ray sent at a small positive elevation angle may actually decrease in height with range and eventually strike the earth. We will demonstrate this in the following sections.

Because the pressure variable usually makes a rather stable contribution to the variation of *N*, we will only analyze the sensitivity of radio refractivity to temperature and moisture. The amount of moisture in the air can be expressed in many forms. Four of the most commonly used moisture variables are dewpoint, T_d, water vapor pressure, relative humidity, and specific humidity. To ease comparisons with the sensitivity to temperature, we will choose the dewpoint as the moisture variable for our sensitivity study. A commonly used approximate relation between dewpoint and water vapor pressure is Teten's formula:

$$e = 6.11\times\exp\frac{\alpha\times(T_d - 273.16)}{T_d - \beta} , \quad (8)$$

where for water, α =17.26, β =35.86 and for ice, α =21.87, β =7.66. Taking the leading-order variation of (8) with respect to dewpoint gives,

$$\delta e = e\times\left(\frac{\alpha\times(273.16-\beta)}{(T_d-\beta)^2}\right)\delta T_d , \quad (9)$$

where δe is the variation of water vapor, *e,* and δT_d is the variation of dewpoint.

By taking the leading-order of variation of the refractivity equation (Eq. 2) with respect to temperature, and water vapor pressure, we have,

$$\delta N = -\left(\frac{77.6P}{T^2} + \frac{2\times 3.73\times 10^5 e}{T^3}\right)\delta T + \frac{3.73\times 10^5}{T^2}\delta e, \quad (10)$$

where δN is the variation of refractivity, and δT is the variation of temperature. Substituting (9) into (10), letting

$$A \equiv \frac{\partial N}{\partial T} = -\left(\frac{77.6P}{T^2} + \frac{2\times 3.73\times 10^5 e}{T^3}\right), \quad (11)$$

$$B \equiv \frac{\partial N}{\partial T_d} = \frac{3.73\times 10^5 (273.16-\beta)\alpha e}{T^2 (T_d-\beta)^2}, \quad (12)$$

and also dividing (10) by δh, we get,

$$\frac{\delta N}{\delta h} = A\frac{\delta T}{\delta h} + B\frac{\delta T_d}{\delta h}. \quad (13)$$

It is obvious from (11) and (12), A<0 and B>0, and normally, both temperature and dewpoint decrease with the height, i.e., $\frac{\delta T}{\delta h} < 0$ and $\frac{\delta T_d}{\delta h} < 0$. So the temperature term makes a positive contribution to the rate of decrease in *N*, but the moisture term makes a negative contribution. To satisfy the condition that the decrease in *N* with height exceeds a certain value (i.e., $\delta N/\delta h$ < -157 km^{-1}), and so that electromagnetic beams are bent toward the surface of the earth, i.e., for them to be trapped, either $\delta T/\delta h$ should be greater than zero (inversion layers exist in the atmosphere), or $\frac{\delta T_d}{\delta h}$ should be much less than zero (a very dry layer overlaying a relatively moist layer).

To quantify our analysis, given a base state with relative humidity RH = 60%, T = 17 °C, and P = 1000 hPa, we can calculate the values of the other base variables T_d = 11.7 °C, e = 13.7 hPa and N = 328.25. Substituting these values into (11) and (12), we get $A \equiv \frac{\partial N}{\partial T} = -1.34$, and $B \equiv \frac{\partial N}{\partial T_d} = 4.02$. These values indicate that a 1 °C change in temperature causes a 1.34 unit change in refractivity; while a 1 °C change in dewpoint causes a 4.02 unit change in refractivity. Since variabilities on the order of few degrees are typical of both temperature and dew point temperature in the lower atmosphere, we can therefore say that the radio refractivity is about three times more sensitive to dew point than temperature near the surface for these typical conditions. This point will be further demonstrated in Section 5. Among a large number of soundings we examined, many of the most extreme deviations of ray paths from the four-thirds earth model are caused by large moisture gradients, usually when a very dry layer is present above a moist boundary layer.

4. A STEPWISE RAY TRACING METHOD

In the last section, we have analyzed the sensitivity of radio refractivity to temperature and dewpoint. To best use the radar data, it is also necessary to examine the influence of different environmental thermodynamic profiles to the radar ray path using actual observed sounding data. To accurately estimate the radar ray path, we develop a stepwise ray tracing method as follows:

(a) Starting from the second gate from radar, for each radar measurement, calculate the refractivity N_{i-1} for the previous gate according to Eq. (2) based on the given thermodynamic profile then calculate the gradient of refractive index according to the differential of Eq. (2) with respect to beam height,

$$\left.\frac{dn}{dh}\right|_{i-1} = 10^{-6}\left.\frac{dN}{dh}\right|_{i-1} \quad (14)$$

here *i* is the index of the gate.

(b) Calculate $a_{e,i-1} = k_{e,i-1}a$ according to Eq. (1) using the gradient of refractive index from step (a) at the last gate, *i-1*;

(c) Calculate the angle between the radar beam and the tangent plane below the data point, $\theta'_{e,i-1}$ using Eq. (6) for each radar beam gate;

(d) Finally, the radar beam height *h* and the surface range *s* for gate *i* can be calculated using the following formulas,

$$h_i = h_{i-1} + \Delta r \times \sin\theta'_{e,i-1}, \quad s_i = s_{i-1} + \Delta r \times cos\,\theta'_{e,i-1}, \quad (15)$$

where, Δr is gate spacing, which is 250 m for U.S. operational WSR-88D (NEXRAD) radial velocity. Variables h_i and s_i are the beam height and surface distance for each gate, respectively. Steps (a) through (d) are repeated for successive gates until the last gate of the radar measurement. Note that within this procedure, we assume that the sounding profile is representative of the vertical structure of the atmosphere within the radar range, which is not always true.

5. PROFILES OF RADIO REFRACTIVITY FOR DIFFERENT GEOGRAPHIC REGIONS

To examine the influence of radio refractivity on the ray path at different geographical regions of the United States, historic sounding data during a six-year period from January 1, 1998 to December 31, 2003 at four different locations are used; namely, Oakland, California (OAK), Key West, Florida (EYW), Dulles Airport, Virginia (IAD) and Topeka, Kansas (TOP). These sites were chosen to represent the West Coast, Tropical Southeast, East-Coast and Great Plains regions of the United States, respectively. Quality-controlled soundings were obtained from the online database of the NOAA Forecast Systems Laboratory.

For each sounding, the radar beam heights at different range gates, for a 0.5º elevation angle beam, are calculated, using Eqs. (3) and (4) with the standard atmosphere condition and using the stepwise method with the actual observed atmospheric profiles. The difference of the beam heights using these two methods is then divided by the corresponding beam width at the corresponding range, assuming a 0.93 degree beam for the U.S. operational radars. The result can be regarded as a relative beam height error. Table 1 shows the distribution of errors among six error intervals for the locations 50 km from the virtual radar site. Among more than 4000 soundings for each sounding site from the 6 years, we find that ray paths determined from the four-thirds earth radius model agree fairly well with the stepwise ray tracing method. More than 90% of the soundings result in relative errors for beam height calculation less than 0.2. Ray paths from four-thirds earth radius model are more accurate with the soundings from Oakland, California (OAK) than that of other sites; no relative errors were greater than 0.8. Ray paths are less accurate with the soundings from Topeka, Kansas, with 0.4 % of soundings whose relative beam height errors are greater than 1.

Table 1. Distribution of relative beam height errors among 6 error intervals for locations 50 km from the radar site.

Raob Sites	Obs. No.	Error Distributions (%)					
		[0 0.2]	[0.2 0.4]	[0.4 0.6]	[0.6 0.8]	[0.8 1.0]	[1.0 above]
OAK	4234	94.31	4.65	0.92	0.12	0.00	0.00
EYW	4202	94.10	5.02	0.79	0.05	0.00	0.05
IAD	4088	97.31	0.86	1.10	0.05	0.44	0.24
TOP	4253	93.63	3.74	1.27	0.75	0.19	0.42

Table 2. Distribution of relative beam height errors among 6 error intervals for locations 120 km from the radar site.

Raob Sites	Obs. No.	Error Distributions (%)					
		[0 0.2]	[0.2 0.4]	[0.4 0.6]	[0.6 0.8]	[0.8 1.0]	[1.0 above]
OAK	4234	76.17	4.82	7.58	10.01	1.42	0.00
EYW	4202	71.68	11.61	7.38	8.02	1.26	0.05
IAD	4088	91.34	3.69	1.71	1.32	1.10	0.83
TOP	4253	86.93	5.48	1.98	2.66	0.59	2.37

Table 2 shows the distribution of errors for the locations 120 km away from the virtual radar sites. For this distance, just over 70 % of soundings result in relative beam height errors less than 0.2 for OAK and EYW. The number of soundings whose beam height errors less than 0.2 is 91.3 % and 86.9 %, for IAD and TOP, respectively, which are better than for OAK and EYW sites, but the number of soundings which result in relative beam height errors above 1.0 are larger, at 0.8% and 2.4%, respectively. As we might expect, range gates further away from the radar sites are

more likely to have larger beam height errors using the four-thirds earth radius model due to the accumulation of error over distance and a greater chance of encountering a layer with an extreme refractivity gradient. Thus radar data far away from radar sites are more prone to have location errors than data closer to radar sites.

From Table 2, we also notice that more than 20% of soundings result in beam height errors between 0.2 and 0.8 for OAK and EYW, but less than 10% for IAD and TOP lie in the same range. No soundings from OAK site, and only 0.05% soundings from EYW whose errors produce relative errors greater than 1.0. However, 0.83% for IAD and 2.37% for TOP result in errors above 1.0. This indicates that while more soundings from IAD and TOP result in accurate ray path calculations based on the simple model, they also give rise to more calculations which have very large relative errors, indicating more variabilities in the vertical refractivity.

Figure 1 show the sounding, refractivity profile and the calculated ray path, for one of the worst cases from OAK. It can be clearly seen that, there is a pronounced temperature inversion and a sharp moisture gradient slightly above the 2 km altitude in Fig. 1a. Consequently, the profile of vertical refractivity gradient has a large deviation of -400 km^{-1} from the Standard Atmosphere condition just above 2 km. The errors for the ray paths are rather small for distances less than 140 km (Fig. 1c), where the beam intersects the inversion layer near 2 km height. In this case, both a temperature inversion and sharp moisture gradient contribute to the large gradient of refractivity. We also examine several of the other cases with large deviations from the four-thirds model (figures not shown) for this site. It is found that in these cases, a temperature inversion and a large moisture gradient usually exist between 1000 hPa and 700 hPa levels, and they cause the beams to become trapped in a layer aloft, but usually not ducted to the ground.

Figure 2 shows the same profiles for one of the worst cases at the TOP site. It is clear that the very strong moisture gradient found in this sounding are responsible for the large refractivity gradient (Fig. 2a, b). The radar beam refracted downward toward the earth surface due to the layer of sharp refractivity gradient below the 1-km level. In this case, the gradient of radio refractivity is largely caused by the vertical variations in humidity. We also examined many of the other cases with large deviations from the four-thirds earth radius model (figures not shown) for this sounding site. It is

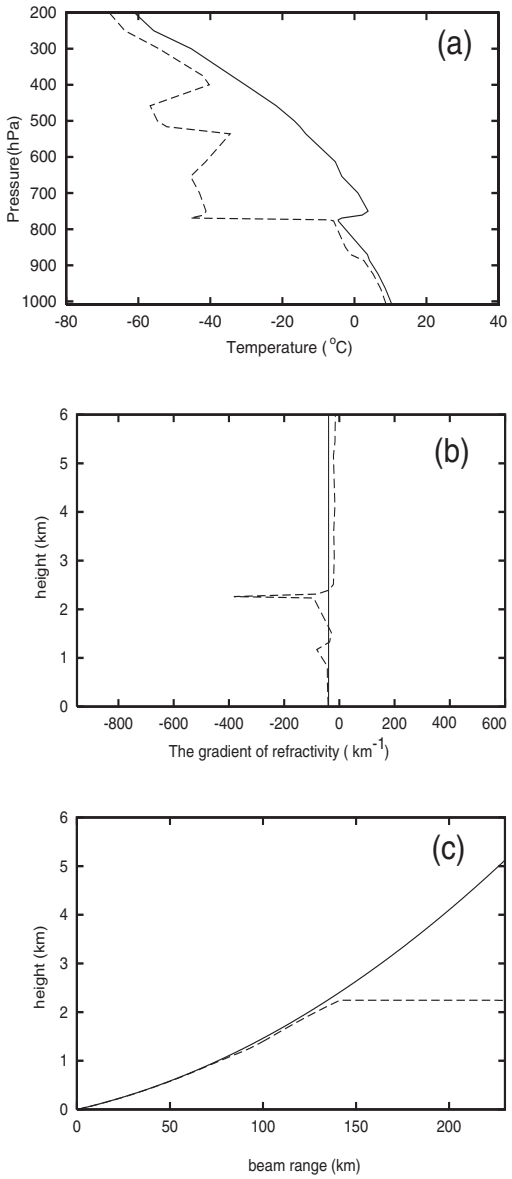

Figure 1. (a) The temperature (solid) and dew point (dashed) profiles, (b) the refractivity gradient profiles (km-1) calculated from the standard atmosphere condition (solid) and from the sounding (dashed),and (c) the radar ray paths calculated for 0.50º elevation angle using the Standard Atmosphere (solid) and actual sounding and ray tracing method (dashed), for 1200 UTC, December 22, 2000 at Oakland California (OAK).

found that in most cases, a large moisture gradient exists at the low levels; these cause the beams to be refracted to the ground at a close distance from the radar (as seen in Fig. 2c). So we notice that the beam ducting phenomena oc-

curs more often in the Great Plains and East Coast areas of the U.S. than in the West Coast or Tropical Southeast because large moisture gradients occur more frequently near the surface. In the Great Plains this situation can be caused by boundary-layer moisture from local sources or advected from the Gulf of Mexico overlaid with dry air having origins from the Rockies to the west. Similarly for Virginia, dry air advected from the Appalachians or with a history of subsidence can be found above a shallow layer of air with origins from the Gulf Stream.

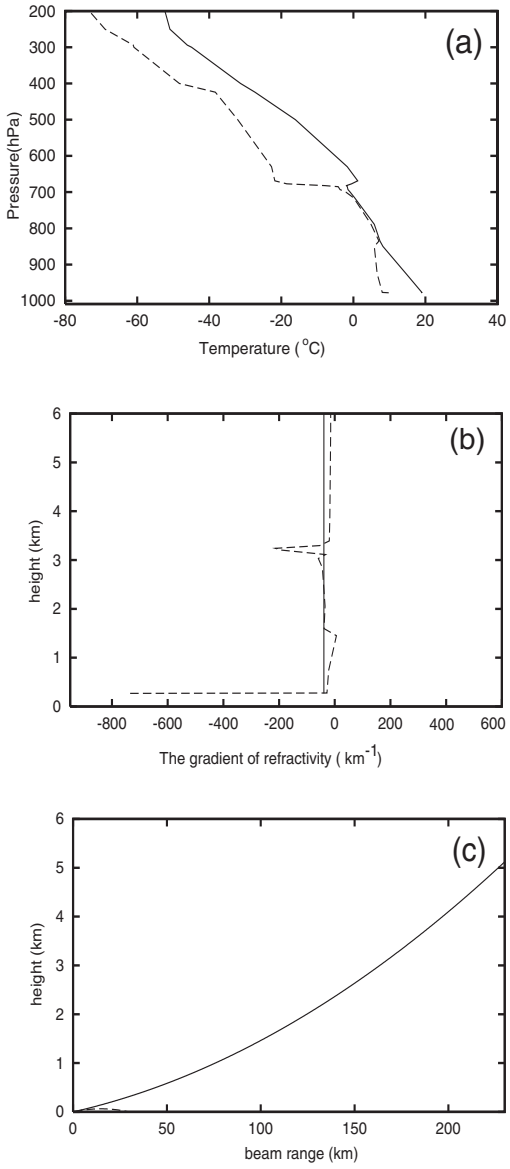

Figure 2. As Figure 1, but for 0000 UTC, May 3, 1999 at Topeka, Kansas (TOP).

Figure 3 shows a recent case study for Amarillo, Texas. A large moisture gradient and temperature inversion near the 1.2 km level (1000 m AGL) are quite pronounced. The calculated beam is trapped in a layer just 1000 m above the ground (Fig 3c). To show the effect on the radar data in this case, Figure 4 shows the radar image at 13:47 UTC, 08 June 2005 for KAMA at Amarillo, Texas. The beam might be partially or completely hitting ground targets in places where you see colors of orange, red or white in the figure. Many pixels within the areas showing high reflectivity have been editing by the clutter filter (black adjacent to red or white areas).

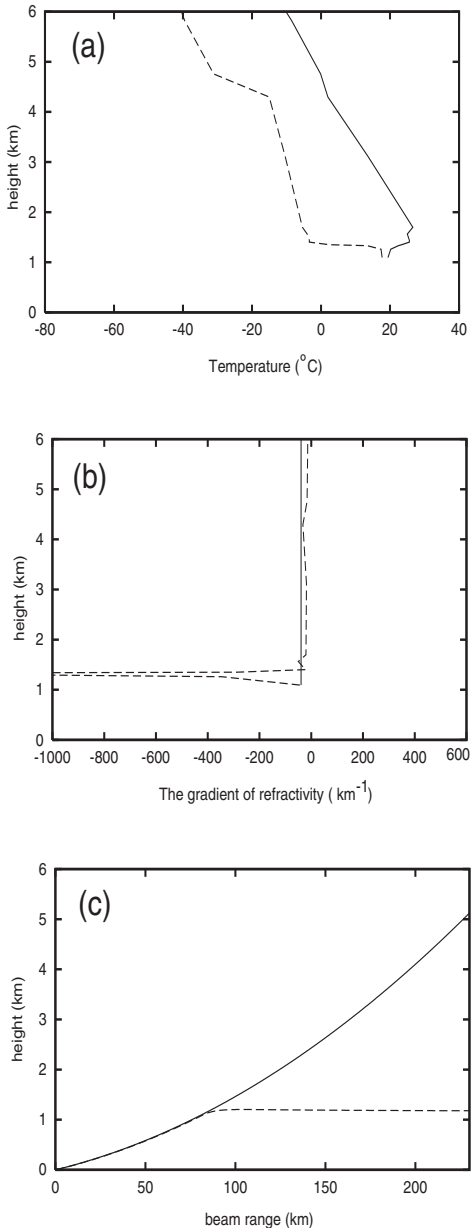

Figure 3. As Figure 1, but for 1200 UTC, June 8, 2005 at Amarillo ,Texas (AMA).

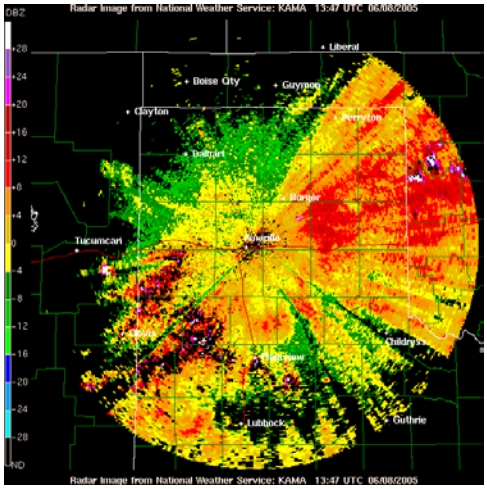

Figure 4. Radar image at 13:47 UTC, June 08,2005 for KAMA at Amarillo, Texas.

Suppose that we require that the error in the beam height relative to the beam width be no more than 0.5 for successful use in data assimilation, then we can see from Tables 1 and 2, that the number of soundings which qualify for the use of the four-thirds earth radius model for the ray path calculation are well above 90%. However, ducting and strong departures from the four-thirds earth model do occur at small percentages, especially in the Great Plains and North-East of United States. These situations are more often related to severe weather events for which the WSR-88D radars are designed. Most of these phenomena are caused by large moisture gradients in the lower atmosphere. For this reason, data assimilation codes should check for such situations and when present use a ray-trace method for beam height calculation and/or discard low-level data that may be contaminated by ground targets due to beam ducting.

6. SUMMARY AND CONCLUSIONS

Radar ray path equations are used to determine the physical location of each radar measurement for use in data display, quality control and data assimilation To best use radar data, the accuracy of ray paths needs to be examined thoroughly to see if significant departures from that calculated under the Standard Atmosphere assumption occur frequently when there are strong temperature inversions and/or large vertical moisture gradient. In this study, we first analyzed the sensitivity of radio refractivity to temperature and moisture. It is found that radio refractivity gradient is more sensitive to the moisture variable, dewpoint than to temperature, so the moisture have a more significant influence on the radar ray path calculation than temperature.

To accurately calculate the radar ray path, a stepwise ray tracing method is developed. The influence of atmospheric refractivity on the ray path for selected geographical locations in the United States is examined using large number of historic soundings from National Weather Service. For the sample of soundings examined at four different geographical locations, we find that 90 % of soundings result in very small relative errors of beam heights when calculated using the simple four-thirds earth radius model based on the Standard Atmosphere and only a small fraction of ray paths thus calculated diverge significantly from those calculated based on a true soundings. But these small fractions of deviations may be more often related to the more important, severe weather situations. For many of the problematic cases examined, the vertical moisture gradient is found to be a more significant contributor. The results of this paper may provide a useful guidance to radar data quality control, and the analysis and assimilation of the data into numerical weather prediction models.

7. ACKNOWLEDGMENTS

This work was supported by NSF grants ATM-0129892, ATM-0331756, ATM-0331594 and EEC-0313747, and DOT-FAA grant NA17RJ1227-01.

8. REFERENCES

Alberty, R. L., T. D. Crum, and F. Toepfer, 1991: The NEXRAD program: Past, present, and future--A 1991 perspective. Preprints, *25th Intl. Conf. on Radar Meteorology*, Paris, Amer. Meteor. Soc., 1-8.

Bean B. R. and E. J. Dutton, 1968: *Radio Meteorology*, Dover Publication, 435 pp.

Brewster, K.A., 2003: Phase-correcting data assimilation and application to storm scale numerical weather prediction. Part II: Application to a severe storm outbreak. *Mon. Wea. Rev.* **131**, 493-507.

Bluestein, H. B. 1993: Synoptic-Dynamic Meteorology in Midlatitudes. Volume II, Oxford University Press, Inc.

Crook, N. A., J. Sun, 2002: Assimilating Radar, Surface, and Profiler Data for the Sydney

2000 Forecast Demonstration Project**.** *J. of Atmos. and Oceanic Technol.*, **19**, 888–898.

Crum, T. D., R. E. Saffle, and J. W. Wilson, 1998: An Update on the NEXRAD Program and Future WSR-88D Support to Operations. *Wea. and Forecasting*, **13**, 253–262.

Doviak, R.J. and D.S. Zrnić, 1993: *Doppler Radar and Weather Observations*, Academic Press, 2nd Edn., 562 pp.

Droegemeier, K. K., 1990: Toward a science of storm-scale prediction. *Preprint, 16th conf. on Severe Local Storms*, Kananaskis Park, Alberta, Canada, Amer. Meteor. Soc., 256-262.

——, 1997: The numerical prediction of thunderstorms: Challenges, potential benefits, and results from real time operational tests. *WMO Bulletin*, **46,** 324-336.

Gao, J**.**, M. Xue, Z. Wang and K. K. Droegemeier, 1998: The initial condition and explicit prediction of convection using ARPS forward assimilation and adjoint methods with WSR-88D data. Preprints, *12th Conference on Numerical Weather Prediction*, Phoenix, AZ, American Meteorol. Society, 176-178.

Gao, J., M. Xue, K. Brewster, and K. K. Droegemeier 2004: A three-dimensional variational data assimilation method with recursive filter for single-Doppler radar, *J. Atmos. Oceanic. Technol.*, **21,** 457-469.

Hu, M., M. Xue, and K. Brewster, 2005a: 3DVAR and Cloud analysis with WSR-88D Level-II Data for the Prediction of Fort Worth Tornadic Thunderstorms. Part I: Cloud analysis and its impact. *Mon. Wea. Rev.***,** Accepted.

Hu, M., M. Xue, J. Gao, and K. Brewster, 2005b: 3DVAR and Cloud analysis with WSR-88D Level-II Data for the Prediction of Fort Worth Tornadic Thunderstorms. Part II: Impact of radial velocity analysis via 3DVAR. *Mon. Wea. Rev.***,** Accepted.

Lilly, D. K., 1990: Numerical prediction of thunderstorms - Has its time come? *Quart. J. Roy. Meteor. Soc.*, **116,** 779-798.

Serafin, R. J., and J. W. Wilson, 2000: Operational Weather Radar in the United States: progress and opportunity. *Bull. Amer. Meteor. Soc*. **81**, 501-518.

Shapiro, A., P. Robinson, J. Wurman, and J. Gao, 2003: Single-Doppler Velocity Retrieval with rapid-scan radar data, *J. Atmos. Oceanic. Technol*. **20**, 1758-1775.

Sun, J., D. W. Flicker, and D.K. Lilly, 1991: Recovery of three-dimensional wind and temperature fields from simulated single-Doppler radar data. *J. Atmos. Sci.,* **48**, 876-890.

Sun, J. and N. A. Crook, 2001: Real-time low-level wind and temperature analysis using single WSR-88D data. *Wea. and Forecasting*., **16**, 117-132.

Weygandt, S.S., A. Shapiro and K.K. Droegemeier, 2002a: Retrieval of initial forecast fields from single-Doppler observations of a supercell thunderstorm. Part I: Single-Doppler velocity retrieval. *Mon. Wea. Rev,* **130**, 433-453.

Weygandt, S.S., A. Shapiro and K.K. Droegemeier, 2002b: Retrieval of initial forecast fields from single-Doppler observations of a supercell thunderstorm. Part II: Thermodynamic retrieval and numerical prediction. Mon. Wea. Rev, 130, 454-476.

Xue, M., D.-H. Wang, J. Gao, K. Brewster, and K. K. Droegemeier, 2003: The Advanced Regional Prediction System (ARPS), storm-scale numerical weather prediction and data assimilation. Meteor. Atmos. Physics. 82, 139-170.